NANO LETTERS

Letter

pubs.acs.org/NanoLett



# In Situ SERS Monitoring of Photochemistry within a Nanojunction Reactor

Richard W. Taylor,[†] Roger J. Coulston,[‡] Frank Biedermann,[‡] Sumeet Mahajan,*[,†] Jeremy J. Baumberg,*[,†] and Oren A. Scherman*[,‡]

[†]NanoPhotonics Centre, Cavendish Laboratory, University of Cambridge, Cambridge, CB3 0HE, United Kingdom

[‡]Melville Laboratory for Polymer Synthesis, Department of Chemistry, University of Cambridge, Cambridge, CB2 1EW, United Kingdom

Supporting Information

**ABSTRACT:** We demonstrate a powerful SERS-nanoreactor concept composed of self-assembled gold nanoparticles (AuNP) linked by the sub-nm macrocycle cucurbit[*n*]uril (CB[*n*]). The CB[*n*] functions simultaneously as a nanoscale reaction vessel, sequestering and templating a photoreaction within, and also as a powerful SERS-transducer through the large field enhancements generated within the nanojunctions that CB[*n*]s define. Through the enhanced Raman fingerprint, the real-time SERS-monitoring of a prototypical stilbene photoreaction is demonstrated. By choosing the appropriate CB[*n*] nanoreactor, selective photoisomerism or photodimerization is monitored in situ from within the AuNP-CB[*n*] nanogap.

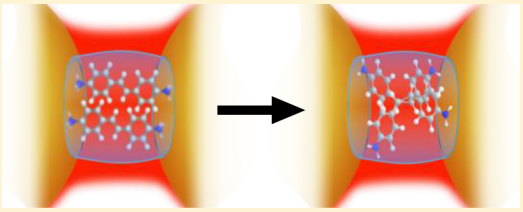

**KEYWORDS:** *Cucurbiturils, gold nanoparticles, diaminostilbene, photoreaction, SERS*

Raman scattering enables molecules to be "fingerprinted" with light and is thus a prominent tool for nondestructive and noninvasive chemical analysis.[1−3] When the target molecule to be detected occurs at trace level (ppb) concentrations, large electromagnetic (EM) amplification to Raman scattering is sought. Nanoscale plasmonic materials are thus widely used to reach the required detection sensitivity.[4−12] Self-assembled clusters of gold nanoparticles (AuNP) provide an attractive general purpose surface-enhanced Raman scattering (SERS) transducer owing to their ease of fabrication,[13] solution processability combined with biological compatibility and chemical inertness,[14−22] and exceptional Raman enhancement.[23−25] Hence Au nanocluster SERS-transducers are finding an increasing role in the fields of biological and chemical sensing as shown in recent reviews,[13,26,27] as well as in frontier fields such as nanomedicine.[28−31]

The extreme EM amplification of SERS by a factor up to $10^{11}$ from plasmonic nanoclusters for SERS-based sensing[24,32−35] facilitates detection down to the single molecule level.[34,36−40] These large optical field enhancements arise from strong confinement of light within the nanojunction crevices between clustered nanoparticles (so-called "hot-spots" of gap plasmons).[41−43] The smallest interparticle gaps yield the highest optical field enhancements and so have become an essential design criteria for applications that require high detection sensitivities.[13] Crucially however, for nanojunctions on the order of a few nanometres or less, the exact particle separation sensitively defines both the coupled plasmon resonance wavelength as well as the SERS enhancement.[44−46] Consequently, the SERS ultimately realized from self-assembled nanoclusters is limited by the extent to which one can control and define the nanojunction spacing.[42] One reason that chemical reactions have not been studied at the single-molecule level is this difficulty of reproducibly constructing nanoscale plasmonic architectures.

Recently, we demonstrated that by using a rigid hollow macrocyclic spacer, known as cucurbit[*n*]uril (CB[*n*], *n* = 5−8,10), the nanojunction spacing between self-assembled gold nanoparticles can be precisely and rigidly fixed to 0.9 nm (Figure 1a).[47−49] The reproducible nanojunction spacing in the AuNP:CB[*n*] nanocluster yields both large optical field enhancements within the nanojunctions in addition to well-defined chain-like plasmon modes that extend across the visible and infrared spectrum.[50,51]

The positioning of the CB[*n*]s directly between the nanoparticles that they separate enables the CB[*n*] to fully experience the enhanced fields during SERS. This is particularly advantageous given that the barrel-shaped CB[*n*] is hollow and so able to sequester molecules within its interior. The CB[*n*] thus doubles as a "reaction vessel" within the nanojunction in which the CB[*n*] may also template the reaction[52−58] and where the contents of the vessel can be probed by SERS.[47,48,59,60] The CB[*n*]-nanojunction reactor thus offers the opportunity not only to sense molecules within CB[*n*] and quantitate them via SERS[59] but also allows for the real-time in situ monitoring of the reaction localized to the nanojunction in

**Received:** August 23, 2013
**Revised:** October 27, 2013
**Published:** November 4, 2013

   dx.doi.org/10.1021/nl403164c | *Nano Lett.* 2013, 13, 5985−5990

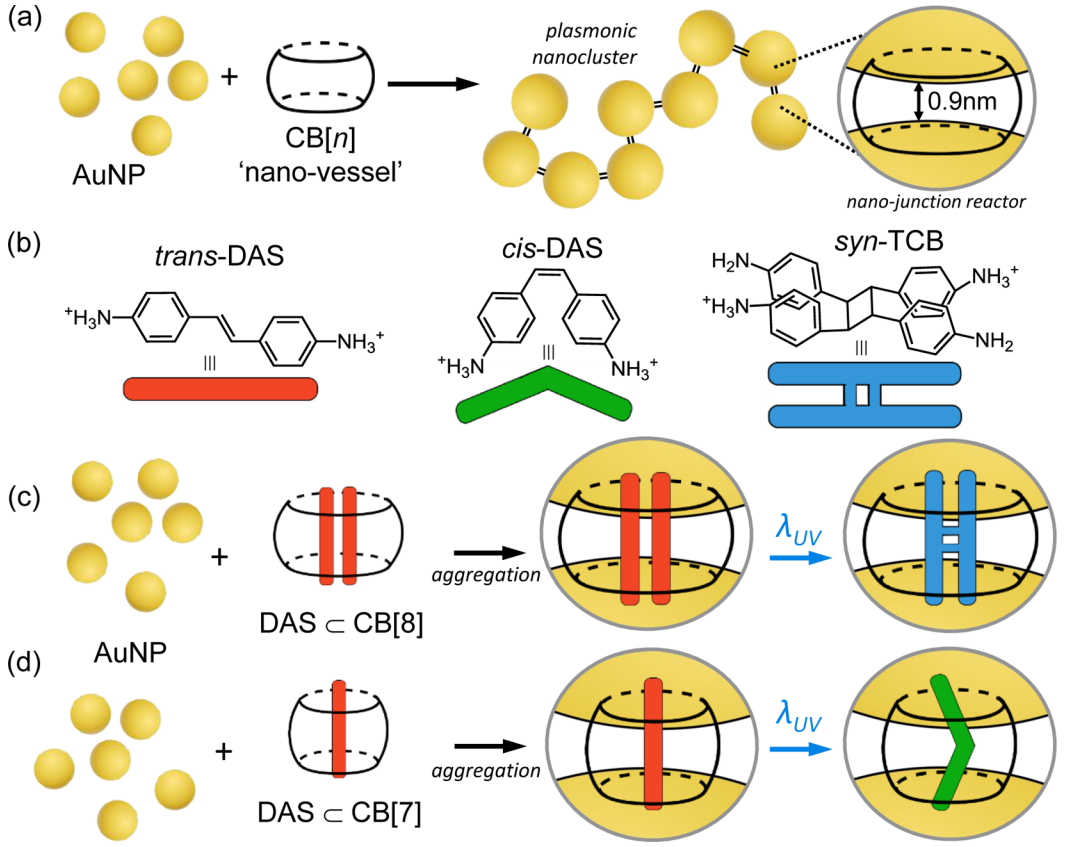


**Figure 1.** (a) AuNPs ($d$ = 60 nm) self-assemble into dendritic nanoclusters with fixed 0.9 nm interparticle separations by the action of the rigid sub-nm CB[$n$] linker. (b) Following UV irradiation in solution, *trans*-DAS predominantly undergoes photoisomerization into *cis*-DAS with photodimerization a minor pathway of which *syn*-TCB is a particular product. (c) When complexed within CB[8], the photoreaction of DAS is templated to yield almost exclusively *syn*-TCB, which can be measured in situ within the interparticle junction of the plasmonic cluster. (d) The complexation of a single DAS within the narrower CB[7] results in a templated photoisomerization reaction to *cis*-DAS.

an aqueous solution. The AuNP-CB[$n$] nanocluster thus serves as a SERS-nanoreactor,[61−63] which is here shown for the first time.

To demonstrate the sensing capability of the AuNP:CB[$n$] SERS-nanoreactor, diaminostilbene (DAS) is chosen as a prototypical aromatic guest molecule because DAS possesses well-known photochemical activity and strong inclusion within CB[$n$]s ($n$ = 7,8).[64,65] The different UV phototransformations of stilbene can be selectively templated by sequestration within the CB[$n$] cavity to yield regioselective photoproducts dictated by the capacity of the cavity, shown in Figure 1. The more voluminous CB[8] forms a 2:1 inclusion complex with DAS and photoirradiation results in [2 + 2] photodimerization of DAS into *syn*-1a,2a,3b,4b-tetrakis(4-aminophenyl)cyclobutane (*syn*-TCB) with high yield (Figure 1c). Alternatively CB[7] forms only a 1:1 complex with DAS, and undergoes trans → cis isomerization upon irradiation (Figure 1d). By constructing such SERS-reactor nanoclusters, we demonstrate the evolution of the two different photoreaction pathways observed through their SERS fingerprint. To provide a sufficiently strong Raman enhancement to monitor the different reactions in the nanojunction, a self-assembled dendritic gold nanoparticle cluster is formed through the aggregation of AuNPs ($d$ = 60 nm) with the CB[$n$] in solution, as reported in our previous work.[47] The plasmon resonance of the AuNP:CB[$n$] aggregates (around $\lambda$ = 800 nm, Supporting Information S1a,b) permits efficient coupling with the Raman excitation wavelength used for SERS ($\lambda$ = 785 nm). A SERS enhancement of ~2 × $10^{10}$ is estimated within the resonant nanojunctions of the nanocluster, comparable to that expected from an optically equivalent nanochain (Supporting Information Figure S1). Such a large SERS enhancement enables the measurement of CB[$n$]-DAS complexes at concentrations of picomole per ml.

The SERS spectra from the CB[8] nanoreactor cluster is shown in Figure 2. A 2:1 DAS ⊂ CB[8] inclusion complex readily forms in solution of which an aliquot is used to induce clustering of AuNPs to yield a SERS spectrum of the

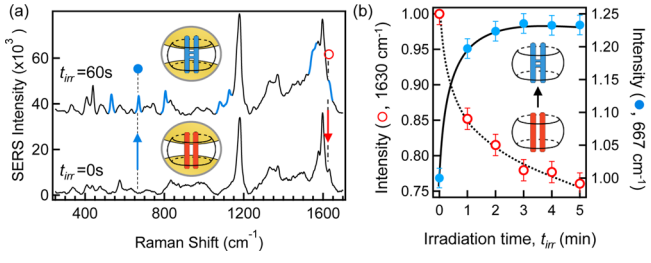


**Figure 2.** (a) SERS spectra of DAS ⊂ CB[8]:AuNP nanocluster solution before ($t_{irr}$ = 0 s) and after ($t_{irr}$ = 60 s) UV irradiation ($\lambda$ = 355 nm). Highlighted modes (blue, $t_{irr}$ = 60 s) indicate newly emergent modes following photocyclisation. Spectra offset and background subtracted for clarity. (b) Time-resolved normalized SERS intensity of the 1630 $cm^{-1}$ alkene mode of the DAS "reactant" (○) and of the 667 $cm^{-1}$ cyclic mode of the *syn*-TCB photocycle product (●). Solid and dashed lines guide the eye.


dx.doi.org/10.1021/nl403164c | *Nano Lett.* 2013, 13, 5985−5990

complexed DAS "reactant" (Figure 2a, $t_{irr}$ = 0 s). In all spectra in Figure 2a, we identify the characteristic Raman modes of the CB[8] with Stokes shift $\nu$ = 440 and 826 cm$^{-1}$, respectively.[60,66] Furthermore, DAS is identified in the spectra by the characteristic C−H in-plane bending and C−C stretching of the benzene rings ($\nu$ = 1179 cm$^{-1}$ and 1550−1600 cm$^{-1}$, respectively) and by the olefin stretching mode ($\nu$ = 1630 cm$^{-1}$).

Complexation of the aromatic stilbene guest within the cavity of CB[8] is evidenced from the increase in frequency of the CB[8] ring breathing deformation mode ($\delta\nu$ = 5 cm$^{-1}$), consistent with recent reports for CB[8] complexed with similar methyl-viologen guests.[59] In the absence of CB[8], the DAS Raman fingerprint is not observed at these ppb concentrations as DAS alone does not strongly bind to the AuNP surface, further emphasizing the importance of the nanovessel/junction-spacer dual role of CB[8].

Irradiation of the DAS ⊂ CB[8]:AuNP nanocluster solution in situ with UV light ($\lambda$ = 355 nm, $t_{irr}$ = 60 s) was found to result in the photodimerization reaction, regioselectively yielding the expected *syn*-TCB ⊂ CB[8] "product" (Figure 2a $t_{irr}$ = 60 s), which was also observed in the absence of AuNP.[52,64] Following irradiation of the nanoreactor cluster, new Raman modes appear that are identified as symmetric and antisymmetric stretching of a cyclic butane ($\nu$ = 1077 and 1127 cm$^{-1}$, respectively), which is a structure unique to the expected *syn*-TCB photoproduct. In addition, further evidence for the cyclobutane product is observed in the series of deformation vibration modes at $\nu$ = 532, 667, and 804 cm$^{-1}$.[67] The benzene ring stretching mode ($\nu$ = 1179 cm$^{-1}$) common to both DAS and the *syn*-TCB product persists unaltered during the reaction, as do the signature modes of CB[8], and so serve as a useful intensity calibration (Supporting Information S2).

In the nanoreactor cluster, the *syn*-TCB product should form at the expense of the initial DAS reactant. Through progressive irradiation ($\Delta t_{irr}$ = 60 s) of the cluster solution, we can use the in situ real time monitoring capability of nanocluster SERS to track the *syn*-TCB production. Figure 2b presents the normalized amplitude for a signature mode of the TCB photoproduct (●, $\nu$ = 667 cm$^{-1}$), which is found to increase with subsequent irradiation and also the simultaneous loss of the DAS measured at the olefin mode (○, $\nu$ = 1630 cm$^{-1}$). Here, both signature modes are normalized to the amplitude of the benzene ring vibration ($\nu$ = 1190 cm$^{-1}$).

We attribute the clarity of the *syn*-TCB photoproduct spectrum in Figure 2a as being due to the remarkable templating of the photoreaction. CB[8] is known to direct DAS photocyclisation to yield the *syn*-TCB isomer with near exclusivity (>95%),[52] all of which occurs within the plasmonic hot-spot of the nanojunction for enhanced detection. The size of the CB[8] cavity favors parallel alignment of the olefins with one-on-one stacking of the benzene rings (*syn*-form). Without the efficient CB[8] templating, photodimerization of DAS would yield multiple isomers resulting in a convoluted SERS spectrum. Furthermore, the dominance of the photodimerization pathway results in the negligible (and unobserved) formation of the alternative photoisomerization of DAS. Given the near exclusive yield of the *syn*-TCB isomer, it is possible that additional changes observed in the SERS spectrum around $\nu$ = 1550 cm$^{-1}$ are due to the "locked" stacking of the benzene rings in the syn- conformation. This arrangement results in a loss of degeneracy for the coupled benzene ring stretches when compared to the unreacted and more mobile sequestered DAS. Cyclisation is however the dominant pathway when templated by CB[8], and trans-to-cis isomerization of the bound DAS would not favor *syn*-TCB.

In addition to using the SERS-nanoreactor concept to monitor a photodimerization reaction, it is also possible to use SERS to monitor changes in molecular conformation via photoisomerization of the reactant in the cluster nanojunction. Using CB[7] as the vessel for the nanoreactor cluster, the CB[7]-photoreaction of DAS follows a trans → cis isomerization, leaving DAS in the cis- configuration within CB[7].[68] The *trans*-DAS ⊂ CB[7]:AuNP complex was formed in the same manner as with CB[8] at neutral pH with the SERS spectrum in Figure 3 (panel a, $t_{irr}$ = 0 s) similarly displaying the

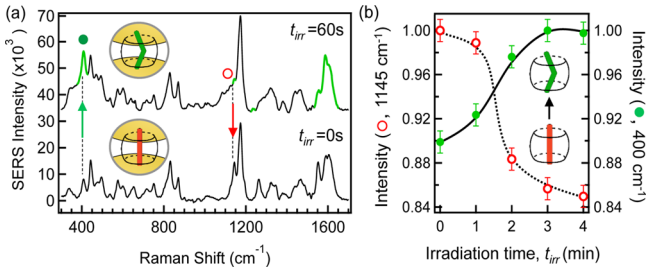


**Figure 3.** (a) SERS spectra of DAS ⊂ CB[7]:AuNP nanocluster solution before ($t_{irr}$ = 0 s, trans-) and after ($t_{irr}$ = 60 s, cis-) UV irradiation ($\lambda$ = 355 nm). Highlighted modes (green, $t_{irr}$ = 60 s) indicate significant amplitude changes following photoisomerization. Complexed DAS concentration 1 nM. Spectra offset and background subtracted for clarity. (b) Time-resolved normalized SERS intensity of characteristic modes for the reactant *trans*-DAS (○) and product *cis*-DAS (●) identified in (a) following subsequent photoirradiation. Solid and dashed lines guide the eye.

Raman signatures of both DAS and CB[7]. The particular ring scissor and ring deformation modes of CB[7] occur at frequencies slightly shifted from that of CB[8] as expected for different CB[*n*] homologoues.[66] Moreover, we similarly identify a shift ($\delta\nu$ = 3 cm$^{-1}$) in the ring deformation mode of CB[7] when complexed with a single DAS guest and also a shift ($\delta\nu$ = 4 cm$^{-1}$) in the benzene ring stretching mode compared to isolated bulk Raman, further confirming incorporation within the CB[7] nanoreactor vessel.

The SERS spectrum of the DAS ⊂ CB[7]:AuNP cluster solution following in situ irradiation is given in Figure 3 (panel a, $t_{irr}$ = 60 s). The spectral signature of the *trans*-DAS reactant [Figure 3 (panel a, $t_{irr}$ = 0 s)] is generally preserved, apart from changes in the relative amplitude of certain modes (highlighted, top spectrum) that evidence isomerization. With the DAS ⊂ CB[7] isomerism reaction, no new chemical bonds are formed, but rather the DAS undergoes a change in conformation.

Upon irradiation, the *trans*-DAS ⊂ CB[7] nanocluster solution exhibits a prominent increase in the $\nu$ = 400 cm$^{-1}$ mode, Figure 3(a,●), tracking torsion about the central alkene bond within the molecule.[67,68] As the steric hindrance is greater in the "twisted" cis form, the amplitude of this torsion mode is expected to increase following trans → cis isomerization, as observed in Figure 3a.[69,70] Moreover, further evidence of the trans → cis conversion is also given by the reduction in the alkene C−H in-plane deformation vibration ($\nu$ = 1145 cm$^{-1}$), which is expected to be less active in the cis conformation.[67] The clarity of the identified changes to these mode amplitudes following photoisomerization is attributed to the trans → cis conversion with CB[7]. When in the cis form, the amine


dx.doi.org/10.1021/nl403164c | *Nano Lett.* 2013, 13, 5985−5990

groups of the complexed DAS are strongly bound to the carbonyl-fringed portals of CB[7], energetically favoring the cis- over the trans- conformation, and thus hindering cis → trans back-conversion.[71,72]

In addition to these identified changes, phototransformation into the cis conformation results in a reorientation of the benzene rings with respect to the CB portal-to-portal (interparticle) axis, as calculated by Kim et al.[68] As CB[$n$] only binds AuNPs through the two carbonyl-fringed portal regions, when pumping the long-wavelength plasmon resonance of the aggregate the highly polarized gap plasmon field in the nanojunctions are always orientated parallel to the portal-to-portal axis. Because of the homogeneous orientation of nanovessels in this gap field, the SERS-nanoreactor is capable of reporting in situ changes in conformation of bound guests, which otherwise would not be possible. The orientation of a benzene ring orthogonal to the gap field when in the cis-conformation, for example, is expected to result in a reduction in the SERS of the associated ring. Indeed, as shown in Figure 3 (panel a, $t_{irr}$ = 60 s), a decrease in the in-plane bending of the benzene ring C−H (○, $\nu$ = 1145 cm$^{-1}$) is observed with UV irradiation. Additional evidence for reorientation of the benzene rings is also given by the prominent change in mode amplitude observed in the $\nu$ = 1550−1600 cm$^{-1}$ region. Progressive irradiation of the DAS ⊂ CB[7] complex (Figure 3b) results in a further reduction in the normalized $\nu$ = 1145 cm$^{-1}$ mode amplitude [Figure 3 (panel b, ○)] along with a proportional increase in the alkene torsional mode (●, $\nu$ = 400 cm$^{-1}$), which confirms the in situ isomerization process from the trans to the cis form.

In addition to identification of the isomerization reaction, we also observe the relatively weak C−O and C−OH (glycol) stretching modes at $\nu$ = 1075 and 600 cm$^{-1}$, respectively. These structures are characteristic of hydrolysis of the stilbene alkene, which is known from photoirradiation of similar aza-stilbenes in water.[73] The cucurbit[$n$]uril interior is hydrophobic[74] and thus shields the olefins of the complexed stilbenes from water. The observation of such hydrolysis products therefore suggests such a photoreaction is able to occur, most likely outside the cavity, in minute quantities, with possible subsequent sequestration into CB[7]. While SERS shows it occurring in low yield, this result opens the possibility for dynamic guest exchange within the nanogap. Notably, we do not observe similar hydrolysis for photoirradiation of the DAS ⊂ CB[8] complex, which is likely due to the remarkable efficiency by which this reaction is templated.

So far we have shown that the photoreactions of DAS may be monitored through the Raman spectral fingerprint using the SERS-nanoreactor cluster. By choice of the CB[$n$] vessel, two different phototransformations of DAS were studied where both could be monitored in situ and in real-time by the nanoreactor cluster. While we estimate quantum yields of around 25% for each reaction, these are hard to evaluate accurately yet. In this final section, we demonstrate the use of CB[8] SERS-nanoreactors to investigate the DAS ⊂ CB[8] supramolecular interaction. The protonated amine groups on the DAS enable the binding interaction with CB[8]. By varying the pH we change the charge interaction between DAS and CB[8] and so the host−guest interaction can be studied through SERS. This investigation is made possible due to the capability of the SERS-nanoreactor cluster to function over a wide pH range (pH 5−11).

The p$K_a$ of the DAS ⊂ CB[8] complex was determined to be 7 (Supporting Information S3). The photodimerization demonstrated for DAS ⊂ CB[8] (Figure 2) was carried out at neutral pH, which leaves the bound DAS monoprotonated ($H_2N$-DAS-$NH_3^+$). The positively charged amines bind strongly to the portals and the pair stack in the "head-to-tail" syn-formation to minimize charge repulsion (Figure 4). The monoprotonation of each of the DAS facilitates photodimerization via what is likely to be intermolecular charge transfer, forming an intermediate excimer complex.[75−77]

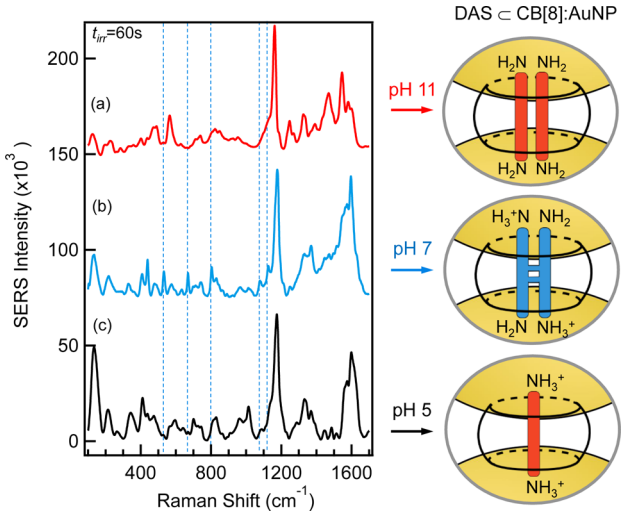


**Figure 4.** SERS intensity of DAS ⊂ CB[8]:AuNP post photoirradiation for three different pH: (a) 11, (b) 7, and (c) 5. Dashed lines guide the eye for the signature photocycle product modes. Spectra offset for clarity. Also shown are schematic illustrations of the DAS ⊂ CB[8] nanocluster particle junctions. The amine groups of the complexed DAS experience varying levels of protonation as a function of pH.

We now consider the photoreaction of the DAS ⊂ CB[8] nanoreactor cluster at different pH values. The post-irradiation SERS spectra ($t_{irr}$ = 60 s) for the different nanoreactor solutions are shown in Figure 4 where in all the spectra we identify the signature modes of CB[8] and DAS.

In basic solution, the DAS amines are uncharged (Figure 4a, pH 11). Although this reduces the binding strength of the complexed pair to the CB[8], the pair are still able to remain bound in a 2:1 stoichiometry since CB[8] is known to complex uncharged guests through the energetically favorable release of high-energy water from the cavity.[78] At this pH, photocyclisation is hindered as the lower association constant suggests that the resonance time of interaction of the DAS pair is lower and also the uncharged amine groups on DAS prevent charge transfer. Accordingly, the SERS spectrum of the DAS ⊂ CB[8] nanoreactor cluster (Figure 4a) shows no signature *syn*-TCB modes previously identified (Figure 4b, blue dash line) consistent with the absence of photocyclisation. The SERS fingerprint in the $\nu$ = 1200−1600 cm$^{-1}$ region is more sharply defined than for other pHs where at least one amine is protonated. This suggests the benzene rings are free to move inside the cavity as the DAS is not "locked" in position within the cavity as with pH 7.

Under more acidic conditions of pH 5, protonation of both DAS amino groups occurs (Figure 4c, pH 5), resulting in charge delocalization across the chromophore. Experimentally


dx.doi.org/10.1021/nl403164c | *Nano Lett.* 2013, 13, 5985−5990

this is seen by an increase in the Raman shift ($\delta\nu$ = 10 cm$^{-1}$) of the alkene stretch mode ($\nu$ = 1600 cm$^{-1}$) and also a shift in the benzene ring mode ($\nu$ = 1125 cm$^{-1}$) than at lower pH.[67] For the fully protonated DAS dication, formation of a 2:1 complex with CB[8] is prevented by the strong charge repulsion between the DAS pair, and as with other dicationic aromatic species, a 1:1 complex is formed exclusively.[79,80] Examination of the SERS spectrum after UV irradiation of the nanoreactor complex at pH 5 similarly reveals the absence of the photocycle product (Supporting Information S4). This result is consistent with the sequestration of a single DAS molecule as the photodimerization of free DAS in water is extremely slow and is not expected to be observed on the time scale of this reaction. Furthermore, there is a relative increase in the alkene torsion mode ($\nu$ = 400 cm$^{-1}$), which is consistent with trans → cis isomerism. It is also of note that the $\nu$ = 1570−1630 cm$^{-1}$ spectral signatures for both the 1:1 DAS ⊂ CB[7] and DAS ⊂ CB[8] complexes following UV-irradiation are similar, suggesting that a trans−cis isomerization also occurs for the 1:1 DAS-CB[8] complex. To further verify our hypothesis of a pH-dependent dimerization reaction, we performed control experiments with a similar but fully methylated, permanently dicationic DAS analogue (bis(*N*,*N*,*N*-trimethyl)-DAS dichloride, Supporting Information S5). This DAS analogue exclusively forms a 1:1 CB[8] complex. We did not find any evidence for photodimerization at any pH in the nanoreactor cluster, thus supporting the interpretation presented above.

**Summary and Conclusion.** In this work, we demonstrate the concept of a SERS-nanoreactor cluster using the capability of CB[*n*] "vessels" to bind AuNPs creating precisely separated hot-spot nanojunctions for sensitive SERS. The CB[*n*] sequesters reactants in its internal cavity and their optimal location within these SERS-active cluster nanojunctions enables photochemical reactions in the cavity to be tracked both in situ and in real-time. Through choice of the smaller and larger homologues CB[7] and CB[8], respectively, the internal volume of the CB[*n*] nanoreactors allows us to obtain direct evidence for photoisomerization and photodimerization using SERS. In addition, we are able to exploit the SERS-nanoreactor motif to explore the role of pH on DAS ⊂ CB[8] host−guest complexation and resultant photoreactions. The flexibility and versatility of the SERS-nanoreactor concept is likely to provide great utility for studying and quantifying different chemical reactions that complex with CB[*n*] and possess distinct Raman spectra.

## ■ ASSOCIATED CONTENT

### Supporting Information

A complementary study using CB[*n*] to template azastilbene photoreactions has also recently been reported by Yang et al.[81] This material is available free of charge via the Internet at http://pubs.acs.org.

## ■ AUTHOR INFORMATION


### Corresponding Authors

*E-mail: (J.J.B.) jjb12@cam.ac.uk.
*E-mail: (S.M.) sm735@cam.ac.uk.
*E-mail: (O.A.S.) oas23@cam.ac.uk.


### Notes

The authors declare no competing financial interest.

## ■ ACKNOWLEDGMENTS

The authors acknowledge the help of Dr. Rubén Esteban for the theoretical calculations of enhancement factors and also useful discussions with Professor Javier Aizpurua and Professor Alex Kuhn. The authors acknowledge Grants UK EPSRC EP/F059396/1, EP/G060649/1 EP/F035535/1, ERC Starting Investigator Grant 240629 (ASPiRe), ERC LINASS 320503 and EP/H007024/1 NanoSci-ERA+ CUBiHOLES.

## ■ REFERENCES


(1) Fleischmann, M.; Hendra, P. J.; McQuillan, A. J. *Chem. Phys. Lett.* **1974**, *26*, 163−166.
(2) Jeanmaire, D. L.; Van Duyne, R. P. *J. Electroanal. Chem.* **1977**, *84*, 1−20.
(3) Albrecht, M. G.; Creighton, J. A. *J. Am. Chem. Soc.* **1977**, *99*, 5215−5217.
(4) Kneipp, K. *Phys. Today* **2007**, *60*, 40.
(5) Alvarez-Puebla, R.; Liz-Marzán, L. M. *Small* **2010**, *6*, 604−610.
(6) Guerrero-Martínez, A.; Grzelczak, M.; Liz-Marzán, L. M. *ACS Nano* **2012**, *6*, 3655−3662.
(7) Moskovits, M. *Rev. Mod. Phys.* **1985**, *57*, 783−826.
(8) Moskovits, M. *J. Raman Spectrosc.* **2005**, *36*, 485−496.
(9) Lim, D.; Jeon, K.; Kim, H. M.; Nam, J.; Suh, Y. D. *Nat. Mater.* **2010**, *9*, 60−67.
(10) Liu, S.; Tang, Z. *J. Mater. Chem.* **2010**, *20*, 24.
(11) Otto, A.; Futamata, M. *Topics in Applied Physics;* Springer-Verlag: Berlin, 2006; Vol. *103*, pp 147−184.
(12) Otto, A.; Mrozek, I.; Grabhorn, H.; Akemann, W. *J. Phys.: Condens. Matter* **1992**, *4*, 1143−1212.
(13) Guerrini, L.; Graham, D. *Chem. Soc. Rev.* **2012**, *41*, 7085−107.
(14) Jin, R. *Angew. Chem., Int. Ed.* **2010**, *49*, 2826−2829.
(15) Song, C.; Wang, Z.; Zhang, R.; Yang, J.; Tan, X.; Cui, Y. *Biosens. Bioelectron.* **2009**, *25*, 826−31.
(16) Vlckova, B.; Gu, X. J.; Moskovits, M. *J. Phys. Chem. B* **1997**, *101*, 1588−1593.
(17) Ghosh, S. K.; Pal, T. *Chem. Rev.* **2007**, *107*, 4797−4862.
(18) Stiles, P. L.; Dieringer, J. A.; Shah, N. C.; Van Duyne, R. P. *Annu. Rev. Anal. Chem.* **2008**, *1*, 601−626.
(19) Etchegoin, P. G. *Phys. Chem. Chem. Phys.* **2009**, *11*, 7348−7349.
(20) Sztainbuch, I. W. *J. Chem. Phys.* **2006**, *125*, 124707.
(21) Sathuluri, R. R.; Yoshikawa, H.; Shimizu, E.; Saito, M.; Tamiya, E. *PloS One* **2011**, *6*, e22802.
(22) Khlebtsov, N. G.; Melnikov, A. G.; Dykman, L. A.; Bogatyrev, V. A. *Optical Properties and Biomedical Applications of Nanostructures Based on Gold and Silver Bioconjugates*; Springer: Netherlands, 2005; Vol. *161*, pp 265−308.
(23) Inoue, M.; Ohtaka, K. *J. Phy. Soc. Jpn.* **1983**, *52*, 3853−3864.
(24) Hao, E.; Schatz, G. C. *J. Chem. Phys.* **2004**, *120*, 357−66.
(25) Xu, H.; Mikael, K. *Estimating SERS Properties of Silver-Particle Aggregates through Generalized Mie Theory*; Springer: New York, 2006; Vol. *104*, pp 87−103.
(26) Alvarez-Puebla, R.; Liz-Marzán, L. M. *Chem. Soc. Rev.* **2012**, *41*, 43−51.
(27) Abalde-Cela, S.; Aldeanueva-Potel, P.; Mateo-Mateo, C.; Rodríguez-Lorenzo, L.; Alvarez-Puebla, R.; Liz-Marzán, L. M. *J. R. Soc. Interface* **2010**, *7*, 435−450.
(28) Gobin, M. A.; Lee, M. H.; Halas, N. J.; James, W. D.; Drezek, R. A.; West, J. L. *Nano Lett.* **2007**, *7*, 1929−1934.
(29) Chen, S.; Svedendahl, M.; Kall, M.; Gunnarsson, L.; Dmitriev, A. *Nanotechnology* **2009**, *20*, 1−9.
(30) Nam, J.; Won, N.; Jin, H.; Chung, H.; Kim, S. *J. Am. Chem. Soc.* **2009**, *131*, 13639−45.
(31) Khlebtsov, B.; Zharov, V.; Melnikov, A.; Tuchin, V.; Khlebtsov, N. *Nanotechnology* **2006**, *17*, 5167−5179.
(32) Ru, E. C. Le; Blackie, E.; Meyer, M.; Etchegoin, P. G. *J. Phys. Chem. C* **2007**, *111*, 13794−13803.

(33) McMahon, J. M.; Henry, A.-I.; Wustholz, K. L.; Natan, M. J.; Freeman, R. G.; Van Duyne, R. P.; Schatz, G. C. *Anal. Bioanal. Chem.* **2009**, *394*, 1819−1825.
(34) Xu, H.; Aizpurua, J.; Kall, M.; Apell, P.; Käll, M. *Phys. Rev. E* **2000**, *62*, 4318−24.
(35) Blaber, M. G.; Schatz, G. C. *Chem. Commun.* **2011**, *47*, 3769−71.
(36) Kneipp, K.; Wang, Y.; Kneipp, H.; Perelman, L. T.; Itzkan, I.; Dasari, R. R.; Feld, M. S. *Phys. Rev. Lett.* **1997**, *78*, 1667−1670.
(37) Nie, S.; Emory, S. R. *Science* **1997**, *275*, 1102−1106.
(38) Dadosh, T.; Sperling, J.; Bryant, G. W.; Breslow, R.; Shegai, T.; Dyshel, M.; Haran, G.; Bar, I. *ACS Nano* **2009**, *3*, 1988−1994.
(39) Aćimović, S. S.; Kreuzer, M. P.; González, M. U.; Quidant, R. *ACS Nano* **2009**, *3*, 1231−1237.
(40) Otto, A.; Mrozek, I.; Grabhorn, H.; Akemann, W. *J. Phys.: Condens. Matter* **1992**, *4*, 1143−1212.
(41) Le Ru, E. C.; Etchegoin, P. G. *Chem. Phys. Lett.* **2004**, *396*, 393−397.
(42) Qin, L.; Zou, S.; Xue, C.; Atkinson, A.; Schatz, G. C.; Mirkin, C. A. *Proc. Natl. Acad. Sci. U.S.A.* **2006**, *103*, 13300−13303.
(43) Li, W.; Camargo, P. H. C.; Lu, X.; Xia, Y. *Nano Lett.* **2009**, *9*, 485−490.
(44) Rechberger, W.; Hohenau, A.; Leitner, A.; Krenn, J. R.; Aussenegg, F. R.; Lamprecht, B. *Opt. Commun.* **2003**, *220*, 137−141.
(45) Atay, T.; Song, J.; Nurmikko, A. V *Nano Lett.* **2004**, *4*, 1627−1631.
(46) Le Ru, E. C.; Etchegoin, P. G. *J. Chem. Phys.* **2009**, *130*, 181101.
(47) Taylor, R. W.; Lee, T.-C.; Scherman, O. A.; Esteban, R.; Aizpurua, J.; Huang, F. M.; Baumberg, J. J.; Mahajan, S. *ACS Nano* **2011**, *5*, 3878−3887.
(48) Tao, C.-A.; An, Q.; Zhu, W.; Yang, H.; Li, W.; Lin, C.; Xu, D.; Li, G. *Chem. Commun.* **2011**, 9867−9869.
(49) An, Q.; Li, G.; Tao, C.; Li, Y.; Wu, Y.; Zhang, W. *Chem. Commun.* **2008**, 1989−1991.
(50) Esteban, R.; Taylor, R. W.; Baumberg, J. J.; Aizpurua, J. *Langmuir* **2012**, *28*, 8881−8890.
(51) Taylor, R. W.; Esteban, R.; Mahajan, S.; Coulston, R.; Scherman, O. A.; Aizpurua, J.; Baumberg, J. J. *J. Phys. Chem. C* **2012**, *116*, 25044−25051.
(52) Jon, S. Y.; Ko, Y. H.; Park, S. H.; Kim, H.-J.; Kim, K. *Chem. Commun.* **2001**, *19*, 1938−1939.
(53) Hwang, I.; Jeon, W. S.; Kim, H.-J. H.; Kim, D.; Selvapalam, N.; Fujita, N.; Shinkai, S.; Kim, K. *Angew. Chem., Int. Ed.* **2007**, *46*, 210−213.
(54) Lee, J. W.; Samal, S.; Selvapalam, N.; Kim, H.-J.; Kim, K. *Acc. Chem. Res.* **2003**, *36*, 621−630.
(55) Mock, W. L.; Irra, T. A.; Wepsiec, J. P.; Adhya, M. *J. Org. Chem.* **1989**, *54*, 5302−5308.
(56) Nau, W. M.; Mohanty, J. *Angew. Chem., Int. Ed.* **2005**, *117*, 3816−3820.
(57) Lagona, J.; Mukhopadhyay, P.; Chakrabarti, S.; Isaacs, L. *Angew. Chem., Int. Ed.* **2005**, *44*, 4844−4870.
(58) Márquez, C.; Hudgins, R. R.; Nau, W. M. *J. Am. Chem. Soc.* **2004**, *126*, 5806−16.
(59) Kasera, S.; Biedermann, F.; Baumberg, J. J.; Scherman, O. A; Mahajan, S. *Nano Lett.* **2012**, *12*, 5924−5928.
(60) Roldán, M. L.; Sanchez-Cortes, S.; García-Ramos, J. V.; Domingo, C. *Phys. Chem. Chem. Phys.* **2012**, *14*, 4935−4941.
(61) Li, J.-F.; Anema, J. R.; Yu, Y.-C.; Yang, Z.-L.; Huang, Y.-F.; Zhou, X.-S.; Ren, B.; Tian, Z.-Q. *Chem. Commun.* **2011**, *47*, 2023−2025.
(62) Li, J. F.; Huang, Y. F.; Ding, Y.; Yang, Z. L.; Li, S. B.; Zhou, X. S.; Fan, F. R.; Zhang, W.; Zhou, Z. Y.; Wu, D. Y.; Ren, B.; Wang, Z. L.; Tian, Z. Q. *Nature* **2010**, *464*, 392−395.
(63) Shi, C.; Zhang, W.; Birke, R. L.; Lombardi, J. R. *J. Phys. Chem.* **1990**, *94*, 4766−4769.
(64) Likhtenshtein, G. I. *Stilbenes: Applications in Chemistry, Life Sciences and Materials Science*; Wiley-VCH Verlag: Weinheim, 2010.
(65) Papper, V.; Likhtenshtein, G. I. *J. Photochem. Photobiol., A* **2001**, *140*, 39−52.
(66) Mahajan, S.; Lee, T.-C.; Biedermann, F.; Hugall, J. T.; Baumberg, J. J.; Scherman, O. A. *Phys. Chem. Chem. Phys.* **2010**, *12*, 10429−10433.
(67) Socrates, G. *Infrared and Raman Characteristic Group Frequencies: Tables and Charts*, 3rd ed.; John Wiley & Sons, Inc.: Chichester, 2010; p 366.
(68) Choi, S.; Park, S. H.; Ziganshina, A. Y.; Ko, Y. H.; Lee, J. W.; Kim, K. *Chem. Commun.* **2003**, *17*, 2176.
(69) Myers, A. B.; Mathies, R. A. *J. Chem. Phys.* **1984**, *81*, 1552.
(70) Choi, C. H.; Kertesz, M. *J. Phys. Chem. A* **1997**, *101*, 3823−3831.
(71) Wu, J.; Isaacs, L. *Chem.—Eur. J.* **2009**, *15*, 11675−11680.
(72) del Barrio, J.; Horton, P. N.; Lairez, D.; Lloyd, G. O.; Toprakcioglu, C.; Scherman, O. A. *J. Am. Chem. Soc.* **2013**, *135*, 11760−11763.
(73) Maddipatla, M. V. S. N.; Kaanumalle, L. S.; Natarajan, A.; Pattabiraman, M.; Ramamurthy, V. *Langmuir* **2007**, *23*, 7545−7554.
(74) Biedermann, F.; Vendruscolo, M.; Scherman, O. A.; De Simone, A.; Nau, W. M. *J. Am. Chem. Soc.* **2013**, *135*, 14879−14888.
(75) Peters, K. S.; Freilich, S. C.; Lee, J. *J. Phys. Chem.* **1993**, *97*, 5482−5485.
(76) Mulliken, R. *J. Am. Chem. Soc.* **1952**, *74*, 811−824.
(77) Mattes, S. L.; Farid, S. *Acc. Chem. Res.* **1982**, *15*, 80−86.
(78) Biedermann, F.; Uzunova, V. D.; Scherman, O. A.; Nau, W. M.; De Simone, A. *J. Am. Chem. Soc.* **2012**, *134*, 15318−15323.
(79) Kim, H.-J.; Heo, J.; Jeon, W. S.; Lee, E.; Kim, J.; Sakamoto, S.; Yamaguchi, K.; Kim, K. *Angew. Chem., Int. Ed.* **2001**, *40*, 1526−1529.
(80) Biedermann, F.; Scherman, O. A. *J. Phys. Chem. B* **2012**, *116*, 2842−2849.
(81) Yang, H.; Liu, L.; Yang, L.; Wang, Z.; Zhang, X. *Langmuir* **2013**, DOI: 10.1021/la4025102.